



SYNTHESIS AND CRYSTAL STRUCTURE OF $\text{LiCuFe}_2(\text{VO}_4)_3$ BY RIETVELD METHOD

A.A. Belik

Department of Chemistry, Moscow State University, 119899, Moscow, Russia

(Refereed)

(Received July 15, 1998; Accepted February 16, 1999)

ABSTRACT

A new triple vanadate $\text{LiCuFe}_2(\text{VO}_4)_3$ was synthesized by a solid-state method. The compound is isotypic with mineral howardite, $\text{NaCuFe}_2(\text{VO}_4)_3$, and crystallizes in a triclinic system (space group $P\bar{1}$ (No. 2); $a = 8.1484(5)$, $b = 9.8024(7)$, $c = 6.6355(4)$ Å, $\alpha = 103.832(3)$, $\beta = 102.353(3)$, $\gamma = 106.975(3)$, $V = 468.68$ Å³, $Z = 2$). Crystal structure of $\text{LiCuFe}_2(\text{VO}_4)_3$ was refined by Rietveld method with $R_{\text{WP}} = 2.32\%$, $R_p = 1.76\%$, $R_I = 2.82\%$, $S = 1.55$, using X-ray diffraction. The crystal structure has five independent cation sites. Lithium cations are located in the cavities $M(1)\text{O}_6$ and $M(5)\text{O}_{10}$, which form infinite chains in the [001] direction and are linked through a common face. The lithium cation in the $M(1)\text{O}_6$ cavity has a square planar coordination. The lithium cation in the $M(5)\text{O}_{10}$ cavity is strongly displaced up to 1.2 Å from the special position (0, 0, 0.5) to a half-occupied general position (0.037, 0.087, 0.40). © 2000 Elsevier Science Ltd

KEYWORDS: A. inorganic compounds, B. chemical synthesis, C. X-ray diffraction, D. crystal structure

INTRODUCTION

The crystal structures of mineral howardite, $\text{NaCuFe}_2(\text{VO}_4)_3$, and the isotypic synthetic compound $\beta\text{-Cu}_3\text{Fe}_4(\text{VO}_4)_6$ are described in the literature [1,2]. Some phosphates, $\text{Fe}_7(\text{PO}_4)_6$ [3], $\text{Mg}_3\text{Ti}_4(\text{PO}_4)_6$ [4], $\text{Zn}_3\text{V}_4(\text{PO}_4)_6$ [5], $\text{Cr}_7(\text{PO}_4)_6$ [6], $\text{Ni}_3\text{Fe}_4(\text{PO}_4)_6$ [7], $\text{Co}_3\text{Fe}_4(\text{PO}_4)_6$ [8], $\text{Co}_7\text{H}_4(\text{PO}_4)_6$ [9], and others, and molybdates, $\text{Ag}_4\text{Zn}_4(\text{MoO}_4)_6$ [10], $\text{Na}_2\text{Mg}_5(\text{MoO}_4)_6$ [11], $\text{NaZn}_{5.5}(\text{MoO}_4)_6$ [12], and others, crystallize in the same structure type. This structure type was first described for $\text{Fe}_7(\text{PO}_4)_6$ [3]. The structural relationships are discussed in detail in ref. 2. This structure type is of interest because it makes it possible to change the cation and anion composition and the number of cations from 6.5 to 8 per unit cell.

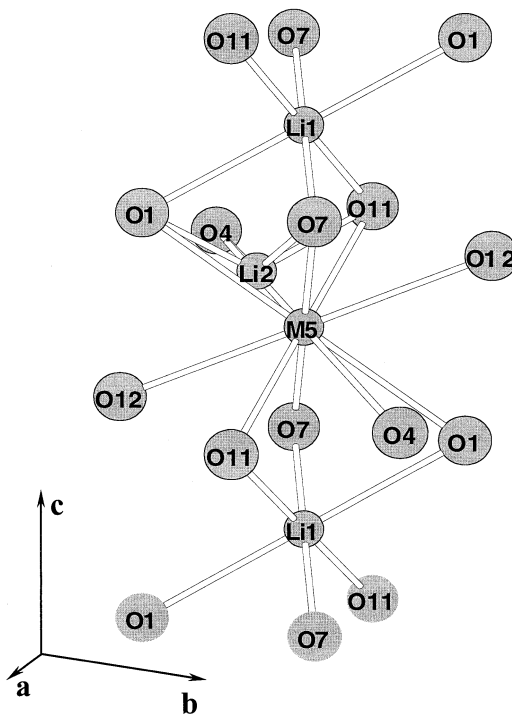


FIG. 1

Oxygen surrounding of lithium cations in the structure of $\text{LiCuFe}_2(\text{VO}_4)_3$. $M(5)$ = ideal position in the center of symmetry; $\text{Li}(2)$ = real position of lithium cation in the $M(5)\text{O}_{10}$ cavity.

Physical properties of these compounds have not been well studied. $\beta\text{-Cu}_3\text{Fe}_4(\text{VO}_4)_6$ is a semiconductor with activation energy ~ 0.20 eV. Below 15 K, $\beta\text{-Cu}_3\text{Fe}_4(\text{VO}_4)_6$ becomes antiferromagnetic [2]. The crystal structure of $\beta\text{-Cu}_3\text{Fe}_4(\text{VO}_4)_6$ has four cation sites: octahedron $M(1)$ and trigonal bipyramidal $M(2)$ for Cu^{2+} ions and two octahedra $M(3)$ and $M(4)$ for Fe^{3+} ions [2]. In the structure of $\text{NaCuFe}_2(\text{VO}_4)_3$ [1], a portion of the sodium cations replaces all the copper cations in octahedron $M(1)$ and another portion of sodium cations is located in the cavity $M(5)$ surrounded by ten oxygen atoms (see Fig. 1). The $M(5)$ cavity is empty in $\beta\text{-Cu}_3\text{Fe}_4(\text{VO}_4)_6$. Sodium cations are displaced from the special position (0, 0, 0.5) and have $\text{CN} = 7$ [1]. Polyhedra of $M(1)\text{O}_6$ and $M(5)\text{O}_{10}$ in $\text{NaCuFe}_2(\text{VO}_4)_3$ [1] link together by a common face and form infinite chains along the [001] direction.

In this paper, the synthesis and crystal structure of a new triple vanadate, $\text{LiCuFe}_2(\text{VO}_4)_3$, are described.

EXPERIMENTAL

Synthesis. $\text{LiCuFe}_2(\text{VO}_4)_3$ was synthesized by solid-state method from a stoichiometric mixture of CuO , Fe_2O_3 , Li_2CO_3 , and V_2O_5 , in a platinum crucible. X-ray phase analysis of a specimen after annealing at 600°C for 50 h showed that it consisted of the expected phase

TABLE 1
Important Counting Conditions and Refined Parameters
for $\text{LiCuFe}_2(\text{VO}_4)_3$

Temperature	297 K
Space group	$P\bar{1}$ (No. 2)
Z	2
2 θ range (°)	8–110
Scan step	0.02
I_{max} (counts)	23271
Lattice constants:	
a (Å)	8.1484(5)
b (Å)	9.8024(7)
c (Å)	6.6355(4)
α	103.832(3)
β	102.353(3)
γ	106.975(3)
V (Å ³)	468.68
Number of Bragg reflections	1174
Structural variables	65
Lattice variables	6
Other variables	15
Reliable factors ^a :	
R_{WP} ; R_P	2.32; 1.76
R_I ; R_F	2.82; 1.82
S	1.55
D-Wd	0.92

^aR factors are defined in ref. 19.

$\text{LiCuFe}_2(\text{VO}_4)_3$ (more than 95 wt%) and impurities of Fe_2O_3 and LiVO_3 . Further annealing at 640°C for 50 h produced a single-phase specimen consisting of very small black crystals. The powder became dark brown after grinding.

Structure Determination. For the structure refinement, an X-ray pattern was obtained using a Siemens D500 powder diffractometer ($\text{Cu K}\alpha_1$ radiation at 30 kV, 30 mA; $\lambda = 1.54060$ Å, SiO_2 monochromator at prime beam, Ni filter, 2 θ range 8–110° with a step interval of 0.02°), equipped with a Braun position sensitive detector. Effective count time per step was ~30 min. The indexing of the powder diffraction pattern of $\text{LiCuFe}_2(\text{VO}_4)_3$ will appear in the Powder Diffraction File. The peak positions and integrated intensities were obtained using the PROFAN program [13]. Indexes hkl were corrected using structure data. The refined cell parameters are $a = 8.1475(6)$, $b = 9.8027(8)$, $c = 6.6348(6)$ Å, $\alpha = 103.838(7)$, $\beta = 102.361(7)$, $\gamma = 106.973(7)$, $V = 468.50$ Å³, $d_x = 3.736$. Figures of merit are $M_{20} = 19.4$, $F_{30} = 41.0$ (0.0163, 45). The difference between the observed and calculated peak positions did not exceed 0.05° in 2 θ .

The crystal structure of $\text{LiCuFe}_2(\text{VO}_4)_3$ was refined by Rietveld method [14], using the RIETAN-97 program [15,16]. The structural parameters of $\text{NaCuFe}_2(\text{VO}_4)_3$ [1] were initially used as the parameters in the crystal structure model of $\text{LiCuFe}_2(\text{VO}_4)_3$. Scattering factors of Li^+ , Cu^{2+} , Fe^{3+} , V , and O^- were used in the refinement. Peak profiles were modeled by a

TABLE 2
Fractional Atomic Coordinates and Isotropic Thermal Parameters for $\text{LiCuFe}_2(\text{VO}_4)_3$

Atom	x/a	y/b	z/c	$B_{\text{iso}} (\text{\AA}^2)$
Li(1)	0	0	0	2(2)
Li(2) ^a	0.037(9)	0.087(9)	-0.60(1)	2.0
Cu	-0.2155(6)	0.2916(5)	0.2730(8)	1.3(2)
Fe(1)	0.4484(7)	0.1079(6)	0.3768(9)	0.1(1)
Fe(2)	-0.2997(6)	-0.4870(5)	0.0456(8)	0.1(1)
V(1)	-0.3980(7)	-0.1641(7)	0.1208(9)	0.7(2)
V(2)	0.2301(7)	0.3780(6)	0.4075(9)	0.9(1)
V(3)	0.1644(7)	-0.2349(6)	0.2303(9)	0.1(1)
O(1)	0.020(2)	0.251(2)	0.302(3)	0.3(1)
O(2)	-0.466(2)	-0.079(2)	0.334(3)	0.3
O(3)	0.284(2)	0.484(2)	0.248(3)	0.3
O(4)	0.320(2)	0.243(2)	0.420(3)	0.3
O(5)	0.256(2)	-0.247(2)	0.460(3)	0.3
O(6)	-0.421(2)	-0.352(2)	0.101(3)	0.3
O(7)	-0.179(2)	-0.071(2)	0.175(3)	0.3
O(8)	-0.501(2)	0.152(2)	0.127(3)	0.3
O(9)	-0.223(2)	0.331(2)	0.058(3)	0.3
O(10)	-0.280(2)	-0.508(2)	0.334(3)	0.3
O(11)	0.192(2)	-0.055(2)	0.223(3)	0.3
O(12)	-0.068(2)	-0.316(2)	0.196(3)	0.3

^aHalf-occupied position with fixed B_{iso} .

modified pseudo-Voight function. The background was refined by a fifth-order polynomial. An overall isotropic thermal factor was used for oxygen atoms. Copper cations were located into the $M(2)$ site. Iron cations were located into the $M(3)$ and $M(4)$ sites. Lithium cations were located into the $M(1)$ and $M(5)$ sites with the center of symmetry at (0, 0, 0) and (0, 0, 0.5). After several cycles of least-squares refinement, it was determined that Li(1) in the $M(1)$ site had $B_{\text{iso}} = 2(2)$ and Li(2) in the $M(5)$ site had $B_{\text{iso}} = 60(5)$ with occupancies of Li(1) and Li(2) positions equal to 1. An unusually large B_{iso} for Li(2) suggested that the atom did not actually lie at the center of symmetry. Thus, the atom was placed in a half-occupied general position. During the refinement of all atom parameters (positional and thermal), it was determined that Li(2) was displaced from the special position up to 1.2 Å and had $B_{\text{iso}} = -2(2)$. The refinement of occupancy gave the value $n = 0.68(8)$ with fixed $B_{\text{iso}} = 2.0$. The displacement of Li(2) cations from special position might result in the loss of the center of symmetry. The refinement in space group $P\bar{1}$ did not improve R-factors. Furthermore, our second harmonic generation study confirmed the centrosymmetric space group for $\text{LiCuFe}_2(\text{VO}_4)_3$. Superstructure reflections that would indicate any regular displacement of Li(2) cations were absent on the X-ray pattern of $\text{LiCuFe}_2(\text{VO}_4)_3$. Thus, Li(2) cations in the $M(5)$ cavity appear to be displaced statistically. The same model was found during single crystal structure refinement of $\text{NaCuFe}_2(\text{VO}_4)_3$ [1] and $\text{Ag}_4\text{Zn}_4(\text{MoO}_4)_6$ [10], which were refined in space group $P\bar{1}$ and in which Na^+ and Ag^+ cations were displaced from the special position to half-occupied general position.

It is common knowledge that there are difficulties in Li localization by powder X-ray

TABLE 3
Important Interatomic Distances (Å) and Angles (°) for $\text{LiCuFe}_2(\text{VO}_4)_3$

Distances and Angles		Distances and Angles	
Li(1)–O(7) (×2)	2.11(2)	Cu–O(9)	1.89(2)
–O(11) (×2)	2.19(2)	–O(5)	1.99(2)
–O(1) (×2)	2.71(2)	–O(1)	2.05(2)
<Li(1)–O>	2.34	–O(10)	2.14(2)
Li(1)–Li(2)	2.52(8)	–O(8)	2.18(2)
Li(1)–O(4) (×2)	3.22(5)	<Cu–O>	2.05
Fe(1)–O(8)	1.91(2)	Fe(2)–O(6)	1.88(2)
–O(4)	1.92(2)	–O(10)	1.95(2)
–O(2)	1.99(2)	–O(12)	1.98(2)
–O(11)	2.08(2)	–O(3)	1.99(2)
–O(2)'	2.12(2)	–O(9)	2.04(2)
–O(5)	2.26(2)	–O(6)'	2.20(2)
<Fe(1)–O>	2.05	<Fe(2)–O>	2.01
Li(2)–O(1)	1.91(7)	V(1)–O(7)	1.66(2)
–O(7)	1.98(7)	–O(8)	1.72(2)
–O(4)	2.33(7)	–O(2)	1.74(2)
–O(11)	2.40(7)	–O(6)	1.76(2)
<Li(2)–O>	2.16	<V(1)–O>	1.72
		O(2)–V(1)–O(6)	112.8(7)
Li(2)–O(7)'	2.87(8)	–O(7)	107.7(8)
Li(2)–O(12)	2.96(8)	–O(8)	113.7(7)
		O(6)–V(1)–O(7)	105.9(7)
		–O(8)	111.0(8)
		O(7)–V(1)–O(8)	105.1(8)
		<O–V(1)–O>	109.4
V(2)–O(1)	1.68(2)	V(3)–O(5)	1.60(2)
–O(3)	1.69(2)	–O(11)	1.73(2)
–O(4)	1.70(2)	–O(12)	1.77(2)
–O(10)	1.76(2)	–O(9)	1.85(2)
<V(2)–O>	1.71	<V(3)–O>	1.74
O(1)–V(2)–O(3)	112.8(7)	O(5)–V(3)–O(11)	115.9(8)
–O(4)	92.4(8)	–O(12)	102.9(8)
–O(10)	115.9(7)	–O(9)	116.2(8)
O(3)–V(2)–O(4)	118.8(7)	O(11)–V(3)–O(12)	103.3(8)
–O(10)	105.1(8)	–O(9)	107.0(8)
O(4)–V(2)–O(10)	112.1(8)	O(12)–V(3)–O(9)	110.8(8)
<O–V(2)–O>	109.5	<O–V(3)–O>	109.4

diffraction. Thus, we refined the structure of $\text{LiCuFe}_2(\text{VO}_4)_3$ in space group $P\bar{1}$ as for $\text{NaCuFe}_2(\text{VO}_4)_3$ and $\text{Ag}_4\text{Zn}_4(\text{MoO}_4)_6$ and in the last refinement cycle the values $n = 0.5$ and $B_{\text{iso}} = 2.0$ were fixed and were not refined for Li(2). We refined only positional parameters for Li(2). The occupancy of Li(2) greater than 0.5 may also indicate that some heavier cations

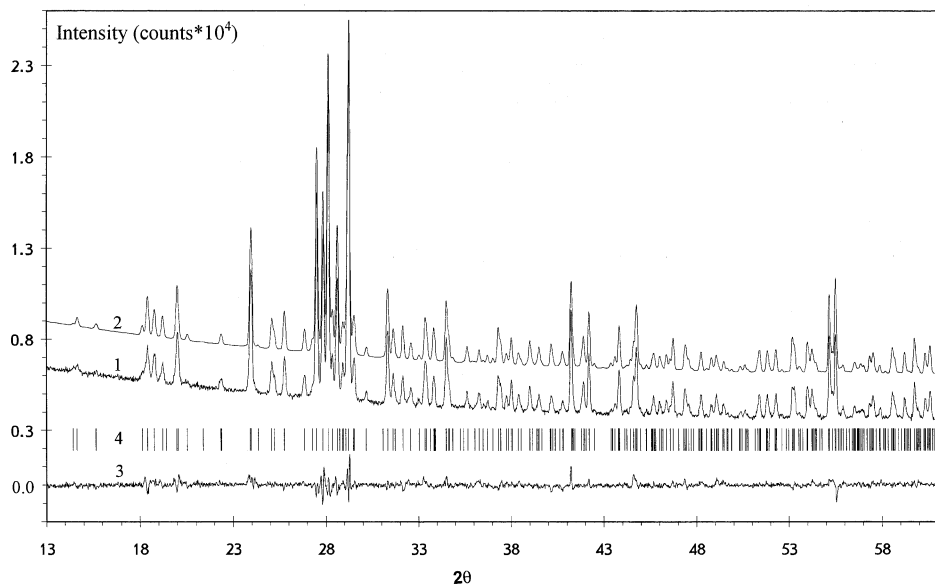


FIG. 2

Portion of the Rietveld refinement profiles for $\text{LiCuFe}_2(\text{VO}_4)_3$; 1 = observed, 2 = calculated, 3 = difference powder X-ray diffraction patterns, and 4 = Bragg reflections. The calculated pattern is shifted to 2500 counts from the observed pattern.

(iron or copper) are localized in the $M(5)$ site. Their quantity is minor, however, since difference in scattering factors for lithium and iron (or copper) is significant.

The details of counting and refinement are given in Table 1. Tables 2 and 3 present the final positional and thermal parameters and important interatomic distances. Figure 2 shows the observed, calculated, and difference patterns for $\text{LiCuFe}_2(\text{VO}_4)_3$.

RESULTS AND DISCUSSION

$\text{Fe}(1)\text{O}_6$, as well as $\text{Fe}(2)\text{O}_6$ octahedra form edge-sharing dimeric clusters. These clusters with surrounding VO_4 tetrahedra form $\text{Fe}(1)_2\text{V}_8$ and $\text{Fe}(2)_2\text{V}_{10}$ units, which create the tridimensional framework [2]. The tridimensional framework $[\text{Fe}_4\text{V}_6\text{O}_{24}]_\infty$ [4,5] creates two types of cavities: [001] tunnels, half-occupied by $\text{Cu}(1)$ ions in $\beta\text{-Cu}_3\text{Fe}_4(\text{VO}_4)_6$ [2] and full-occupied by $\text{Na}(1)$ and $\text{Na}(2)$ ions in $\text{NaCuFe}_2(\text{VO}_4)_3$ [1], and, also along this direction, $\text{Cu}(2)$ sites containing fivefold-coordinated Cu^{2+} ions in both $\beta\text{-Cu}_3\text{Fe}_4(\text{VO}_4)_6$ and $\text{NaCuFe}_2(\text{VO}_4)_3$. The interatomic distances in the framework polyhedra $\text{Fe}(1)\text{O}_6$, $\text{Fe}(2)\text{O}_6$, and $\text{V}(1,2,3)\text{O}_4$, as well as in CuO_5 , are very close for the three structures.

Table 4 presents interatomic distances for $\beta\text{-Cu}_3\text{Fe}_4(\text{VO}_4)_6$, $\text{NaCuFe}_2(\text{VO}_4)_3$, and $\text{LiCuFe}_2(\text{VO}_4)_3$ structures in the cavities $M(1)\text{O}_6$ and $M(5)\text{O}_{10}$ formed by tridimensional framework $[\text{Fe}_4\text{V}_6\text{O}_{24}]_\infty$. The average $M(1)\text{-O}$ and $M(5)\text{-O}$ distances are changed regularly in accordance with cation type located in the $M(1)$ and $M(5)$ sites. The average $M(1)\text{-O}$ distance increases in the series Cu-Li-Na, because the radius of cation located in this site

TABLE 4
Interatomic Distances (Å) in the $M(1)\text{O}_6$ and $M(5)\text{O}_{10}$ cavities in $\beta\text{-Cu}_3\text{Fe}_4(\text{VO}_4)_6$,
 $\text{NaCuFe}_2(\text{VO}_4)_3$, and $\text{LiCuFe}_2(\text{VO}_4)_3$

Distances	$\text{LiCuFe}_2(\text{VO}_4)_3$	$\text{NaCuFe}_2(\text{VO}_4)_3$	$\beta\text{-Cu}_3\text{Fe}_4(\text{VO}_4)_6$
$M(1)\text{-O}(7)$ ($\times 2$)	2.11(2)	2.190(4)	1.955(8)
-O(11) ($\times 2$)	2.19(2)	2.295(4)	2.069(14)
-O(1) ($\times 2$)	2.71(2)	2.860(4)	2.758(14)
$\langle M(1)\text{-O} \rangle_{[6]}$	2.34	2.448	2.261
$M(5)\text{-O}(7)$ ($\times 2$)	2.15	2.29	2.39
-O(11) ($\times 2$)	2.71	2.70	2.75
-O(1) ($\times 2$)	3.03	3.12	3.08
-O(12) ($\times 2$)	3.08	3.20	3.15
$\langle M(5)\text{-O} \rangle_{[8]}$	2.74	2.83	2.92
-O(4) ($\times 2$)	3.21	3.37	3.47
$\langle M(5)\text{-O} \rangle_{[10]}$	2.84	2.94	2.97

increases ($r_{\text{VI}}(\text{Cu}^{2+}) = 0.73$ Å, $r_{\text{VI}}(\text{Li}^+) = 0.74$ Å, $r_{\text{VI}}(\text{Na}^+) = 1.02$ Å [17]). The average $M(5)\text{-O}$ distance decreases in the series Cu–Na–Li because this site is vacant in $\beta\text{-Cu}_3\text{Fe}_4(\text{VO}_4)_6$ that results in the repulsion of oxygen atoms and Na^+ radius is greater than Li^+ radius. Provided by the tridimensional framework, the $M(1)\text{O}_6$ and $M(5)\text{O}_{10}$ cavities are very close to each other in the three structures. Since $d(\text{Li}(1)\text{-O}(1)) = 2.71(2)$ Å is considerably greater than $d(\text{Li}(1)\text{-O}(7)) = 2.11(2)$ Å and $d(\text{Li}(1)\text{-O}(11)) = 2.19(2)$ Å and greater than usually observed Li–O distances 2.00–2.41(4) Å (CN = 6) [18], Li(1) cations have a square planar oxygen surrounding (Fig. 1) like Cu(1) cations in $\beta\text{-Cu}_3\text{Fe}_4(\text{VO}_4)_6$ [2]. The interatomic distances in the $M(5)\text{O}_{10}$ cavity are too large for Li^+ cations (Table 4). Thus, Li(2) cations are displaced up to 1.2 Å from the special position $M(5)$ (0, 0, 0.5) to a half-occupied general position and “cling” to the face O(1)–O(4)–O(11)–O(7) (Fig. 1). The doubled distance between Li(2) cation and the ideal $M(5)$ site (2.4(2) Å) is close to the Li(1)–Li(2) distance (2.52(8) Å). The distance between Li(1) cation and the ideal $M(5)$ site is 3.32 Å (c/2).

The cavities $M(1)\text{O}_6$ and $M(5)\text{O}_{10}$ are linked through the common face O(1)–O(7)–O(11) (Fig. 1). Cations with radius 0.46 Å can freely pass through this face (radius of oxygen is

TABLE 5
Unit-cell parameters for $\beta\text{-Cu}_3\text{Fe}_4(\text{VO}_4)_6$, $\text{NaCuFe}_2(\text{VO}_4)_3$, and $\text{LiCuFe}_2(\text{VO}_4)_3$

Compound	a , Å	b , Å	c , Å	α	β	γ	V , Å ³	Ref.
$\beta\text{-Cu}_3\text{Fe}_4(\text{VO}_4)_6$	8.048	9.759	6.600	103.72	102.28	106.08	461.9	[2]
	8.0570	9.7472	6.6006	103.792	102.204	105.980	461.9	^a
$\text{NaCuFe}_2(\text{VO}_4)_3$ howardite	8.198	9.773	6.6510	103.82	101.99	106.74	473.1	[1]
$\text{LiCuFe}_2(\text{VO}_4)_3$	8.1484	9.8024	6.6355	103.832	102.353	106.975	468.7	^a

^aResults from present Rietveld processing of X-ray patterns.

equal to 1.4 Å [17]). Cations with a radius of 0.56 Å and 0.48 Å can pass freely through this face in, respectively, $\text{NaCuFe}_2(\text{VO}_4)_3$ and $\beta\text{-Cu}_3\text{Fe}_4(\text{VO}_4)_6$.

Table 5 gives the cell parameters for $\beta\text{-Cu}_3\text{Fe}_4(\text{VO}_4)_6$, $\text{NaCuFe}_2(\text{VO}_4)_3$, and $\text{LiCuFe}_2(\text{VO}_4)_3$. As can be seen, the replacement $\text{Cu}^{2+} \rightarrow 2M^+$ ($M = \text{Li}^+, \text{Na}^+$) leads to increase of the unit-cell volume. This indicates that the size of the $M(1)$ cavity affects the unit-cell volume more strongly than does the size of the $M(5)$ cavity.

It is worth noting that, because $\beta\text{-Cu}_3\text{Fe}_4(\text{VO}_4)_6$ and $MCuFe_2(\text{VO}_4)_3$ ($M = \text{Li}^+, \text{Na}^+$) are isotopic, the solid solutions $M_{2x}\text{Cu}_{3-x}\text{Fe}_4(\text{VO}_4)_6$ ($M = \text{Li}^+, \text{Na}^+; 0 \leq x \leq 1$) must exist with different occupancies of the $M(1)$ and $M(5)$ cavities by Cu^{2+} and M^+ cations.

ACKNOWLEDGMENTS

This work was supported by the Russian Fundamental Research Foundation (No. 97-03-33224a).

REFERENCES

1. J.M. Hughes, J.W. Drexler, C.F. Campana, and M.L. Malinconico, *Am. Mineral.* **73**, 181 (1988).
2. M.A. Lafontaine, J.M. Grenache, Y. Laligant, and G. Ferey, *J. Solid State Chem.* **108**, 1 (1994).
3. Yu.A. Gorbunov, B.A. Maksimov, Yu.K. Kabalov, A.N. Ivaschenko, O.K. Mel'nikov, and N.V. Belov, *Dokl. Akad. Nauk SSSR* **254**, 873 (1980).
4. A. Benmoussa, M.M. Borel, A. Grandin, A. Leclaire, and B. Raveau, *J. Solid State Chem.* **84**, 299 (1990).
5. S. Boudin, A. Grandin, A. Leclaire, M.M. Borel, and B. Raveau, *J. Solid State Chem.* **115**, 140 (1995).
6. R. Glaum, *Z. Kristallogr.* **205**, 69 (1993).
7. A. El Kira, R. Gerardin, B. Malaman, and C. Gleitzer, *Eur. J. Solid State Inorg. Chem.* **29**, 1119 (1992).
8. P. Lightfoot and A.K. Cheetham, *J. Chem. Soc., Dalton Trans.*, 1765 (1989).
9. P. Lightfoot and A.K. Cheetham, *Acta Crystallogr. C* **44**, 1331 (1988).
10. C. Gicquel-Mayer, M. Mayer, and G. Perez, *Acta Crystallogr. B* **37**, 1035 (1981).
11. R.F. Klevtsova, V.G. Khim, and P.V. Klevtsov, *Kristallografiya* **25**, 1148 (1980).
12. C. Gicquel-Mayer and M. Mayer, *Rev. Chim. Miner.* **20**, 88 (1983).
13. L.G. Akselrud, Yu.N. Gryn, P.Yu. Zavalij, V.K. Pecharsky, and V.S. Fundamensky, in *Abstracts of Papers: 12th European Crystallography Meeting, Moscow*, Vol. 3, p. 155 (1989).
14. H.M. Rietveld, *Acta Crystallogr.* **22**, 151 (1967).
15. F. Izumi, in *The Rietveld Method*, ed. R.A. Young, pp. 236–253, Oxford University Press, New York (1993).
16. Y.-I. Kim and F. Izumi, *J. Ceram. Soc. Jpn.* **102**, 401 (1994).
17. R.D. Shannon, *Acta Crystallogr. A* **32**, 751 (1976).
18. *International Tables for X-ray Crystallography*, Vol. 3, p. 258, Kynoch Press, Birmingham, UK (1969).
19. R.A. Young, *The Rietveld Method*, Oxford University Press, New York, 1993.